Journal of Applied Geodesy 2 (2008), 131–137 © de Gruyter 2008. DOI 10.1515/JAG.2008.015

A correlation based target finder for terrestrial laser scanning

Thomas Abmayr, Franz Härtl, Gerd Hirzinger, Darius Burschka and Christoph Fröhlich

Abstract. Many calibration and registration methods for optical sensors require highly accurate and robust detection of markers. To date, many different approaches for detecting markers have been developed. However, all of these share certain disadvantages, depending on the optical sensor and their application. We have developed a novel approach for high-accuracy target point detection based on normed cross-correlation from symmetric patterns.

The method has been specifically developed for terrestrial laser scanning, but may also work for other types of optical sensors due to its vision based properties. Our method is robust to noise and invariant to rotation, translation and perspective projection. It is scale invariant and also works in varying distances. In addition, the cross-correlation function allows quality control. Another advantage of this method is that only a few parameters need to be adjusted. Consequently, it is applicable in field test scenarios. The method does not require a certain target pattern. The only constraint on the target type is that after projecting it perspectively, a region around the target center has to remain symmetric and the approximate position of the target center has to be known. Our results demonstrate the robustness and accuracy of this method which we have validated in field applications.

Keywords. Terrestrial laser scanning, sub-pixel accuracy, target detection, cross-correlation.

1. Introduction

To date, a number of approaches for fitting targets have been developed and several different target pattern are currently in use. Among those, circles and chess-patterns are the most common, however they were primarily developed and validated for camera-based applications. In general, different optical sensors vary in their measurement characteristics, which results in different behavior of the sampled data. For example, laser scanners tend to blur edges more than cameras. Therefore, it cannot be generally stated that methods suited for one type of sensor are also qualified for other sensors. Furthermore, these methods are often developed for only one specific application. For example in camera calibration, they are often applied only in a certain range and by using standardized illumination conditions.

The methods can be categorized into three classes, independent of the pattern:

Gradient based methods: They gather necessary information by using the derivative of the image, e.g. several corner detection methods (Förstner and Gülch 1987, Intel 2005) and most circle-fit methods (Bookstein 1988, Fitzgibbon and Fisher 1995). *Curvature based methods*: These methods use the eigenvectors of the Hessian matrix of the intensity image to calculate the most significant increase of the gray-values, e.g. Harris' (Harris and Stephens 1988) and KLT (Shi and Tomasi 1994) corner detectors are based on this principle. *Intensity based methods*: Cross-correlation of a region of interest and a mask image are most commonly used. The powerful image matching techniques (see Gruen 1985, Ackermann 1984) also belong in this category. As correlation-based methods gather the information of each pixel, they are also named *region based methods*.

Each of these methods has certain disadvantages depending on the optical sensor and its application: circle based methods are theoretically the most accurate, but they are not invariant under perspective projection. Furthermore, these methods are mostly gradient based and may thus not be the best choice for laser scanner sensors (see above). In addition many gradient based methods need a threshold for the detection of the circle-edge. This is often difficult to determine because of varying distances and illuminations of the markers in many field applications.

In contrast, corner based methods face the problem that their feature value only is based on a small neighborhood around each pixel. Consequently, local optima can exist and thus the target center often can not be detected robustly. These approaches therefore lack their robustness in varying distances and rotations.

Finally, correlation based methods are in general not invariant to rotation, scaling and perspective projection and image matching is time consuming.

Applications in terrestrial laser scanning have to be able to fit markers with highest accuracy, combined with robustness to varying distances and rotation (see Figure 1). Our method is based on correlation: the main concept is to correlate the input image with a search window as in all correlation based approaches. But opposite to most currently applied methods, we obtain the search window by only using the input image and not by using a predefined mask: Our mask image equals the region of interest rotated by 180 degrees. If a pattern is symmetric with respect to a certain point, this point is uniquely defined. This relationship and its uniqueness will be derived and proven in the paper.

Our approach is not based on a certain target pattern: the only constraint on the target type is that

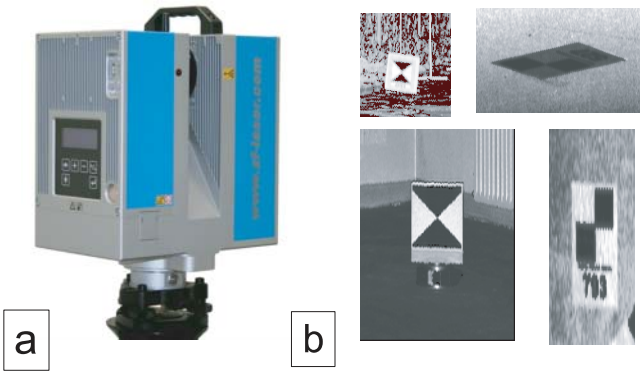

Figure 1: (a) The Zoller and Fröhlich laser scanner Imager 5006; (b) The reflectance image of several markers scanned in different distances and orientations.

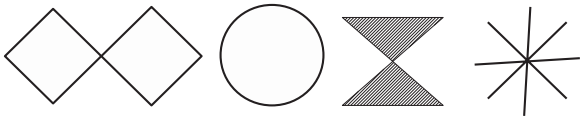

Figure 2: Examples of symmetric targets.

after projecting it perspectively, a region around the target center has to remain symmetric (see Figure 2).

Sub-pixel accuracy is achieved by fitting the output image of the cross-correlation with polynomials of degree two. This approximation is very robust and accurate as the correlation image has only one maximum. Additionally, the correlation based character of the approach could be used as a good quality criteria of the result.

The outline of the paper is as follows: First, we give an introduction into the mathematical background of the approach, and prove the main idea behind the method. Then, we introduce some aspects of the implementation and realization and close with experimental results.

2. Mathematical background

We start with some important definitions and notations.

2.1. Definitions

The first definition introduces a class of targets which we call "symmetric targets".

Denote[1]

$$G := (g_{ij})_{i \le N, j \le M} \tag{1}$$

the matrix of grey values of an image and $A_{m,n} : \mathbb{R}^2 \to \mathbb{R}^2$ with

$$A_{m,n}(x, y) = (2m - x, 2n - y) \tag{2}$$

a 2D point reflection at the center (m, n). Now define the matrix of the transformed image G^* through

$$G^* := (G(A_{m,n}(i, j)))_{i \le N, j \le M}. \tag{3}$$

If $G = G^*$ then G is symmetric with respect to the center of the point reflection $A_{m,n}$ and is called a *symmetric target* (see Figure 2). Then $N = M$ and $(m, n) = \left(\frac{N}{2}, \frac{N}{2}\right)$.

The reflection $A_{m,n}$ is invariant to translation in the sense, that a given set of points can either *first* be reflected on the reflection center (m, n) and *then* be translated, or the reflection center can *first* be translated and *then* the set of points be reflected. This may be clear intuitively but is very important for the realization of our method, and so we will now formalize this matter.

2.2. Invariance property of $A_{m,n}$

Given is the reflection A and two centers (m, n) and (p, q). Then there exists a translation $t \in \mathbb{R}^2$ so that for all $(x, y) \in \mathbb{R}^2$

$$A_{m,n}(x, y) = A_{p,q}(x, y) + t. \tag{4}$$

Proof. To show this choose any $(x, y) \in \mathbb{R}^2$ and set $t = 2(m - p, n - q)$. Then $A_{p,q}(x, y) + t = (2p - x + 2(m - p), 2q - y + 2(n - q)) = (2m - x, 2n - y) = A_{m,n}(x, y)$. □

We will now show how this property can be used to calculate the target center.

2.3. Calculating the target center

Given is the set of pixel indices around the searched target center (m, n) through

$$I := \{(m - k, n - l), \ldots, (m + p, n + q)\} \tag{5}$$

and the sub matrix H of the symmetric target G (see Figure 3) through

$$H := (G_{ij})_{(i,j) \in I}. \tag{6}$$

Let H be uniquely defined in G, i.e. there exists no second submatrix H' of G with $H = H'$. Denote the center of H with (r_1, s_1).

If we assume for now to know the searched target center point (m, n) then we can construct a second sub matrix through

$$H^* := (G(A_{m,n}(i, j)))_{(i,j) \in I} \tag{7}$$

which holds $H^* = H(A_{m,n})$ for all $(i, j) \in I$. And in particular (r_1, s_1) is mapped to $(r_2, s_2) := A_{m,n}(r_1, s_1)$ and thus

$$(m, n) = \frac{1}{2}(r_1 + r_2, s_1 + s_2). \tag{8}$$

1 Throughout this paper we use the following notation to describe the gray values of an image G: Denote N the width and M the height of G, then we define G through: $G := (g_{ij})_{i \le N, j \le M}$.

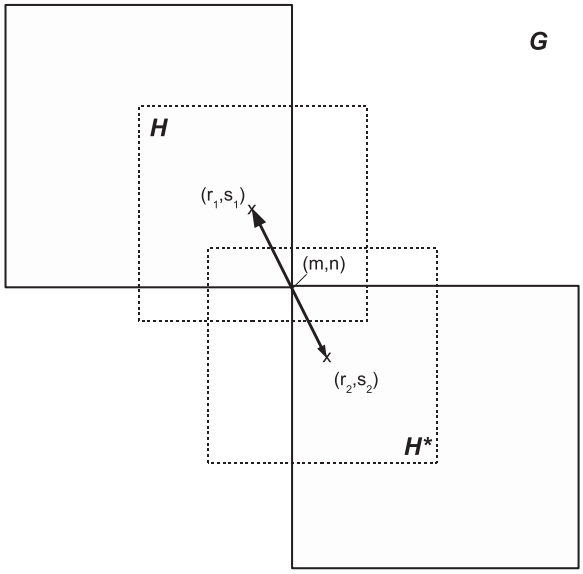

Figure 3: Subset H and the location of its center (r_1, s_1) and H^* and (r_2, s_2) respectively, with respect to the center (m, n) of a symmetric target G.

H and its center (r_1, s_1) are known by construction, but as (m, n) is unknown, H^* and (r_2, s_2) are also unknown. But by using (4) we know that we can construct a set of points which equals H^* through

$$\tilde{H}^* := (H(A_{r_1,s_1}(i,j)))_{(i,j)\in I}. \tag{9}$$

Then $H^* = \tilde{H}^*$. If we now denote the indices of G with I_G and of $\tilde{H}^*$ with $I_{\tilde{H}^*}$ respectively then we can calculate a feature image C (see Figure 5 (4)) by convolving $\tilde{H}^*$ over G and calculate for each index $(i, j) \in I_G$ the normalized cross-correlation value through

$$C_{ij} := \sum_{(k,l)\in I_{\tilde{H}^*}} \frac{(G_{ij} - \bar{G})(\tilde{H}^*_{kl} - \bar{H})}{\bar{G}\bar{H}}. \tag{10}$$

C will be maximal at the index (i, j) where G and $\tilde{H}^*$ match best and thus (r_2, s_2) is calculated through

$$C_{r_2,s_2} := \max(\ldots, C_{ij}, \ldots). \tag{11}$$

So finally by using equation (8) we get the target center (m, n).

Furthermore, the normalized cross-correlation value C_{ij} can be used as simple but effective cross-check of the quality and coherence of the result.

The target we used for our experimental setup was a chess-pattern type (see Figure 4): We decided for this type because its pattern is symmetric (in the sense we introduced in this section) and unlike some other targets holds this property also under perspective projection. We give a prove of this in the appendix. But we also decided to choose this target, because for this target type already several methods exist. This gives us a good chance to cross-check our method.

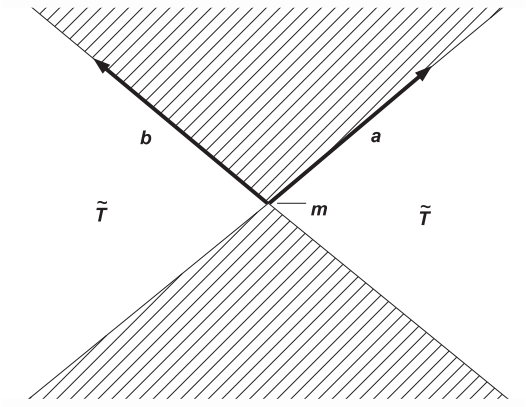

Figure 4: A type of symmetric target which also holds this property under perspective projection.

3. Aspects of the implementation

Up to now, the theoretical background of the target finder detection was shown. In this section, aspects of the implementation will be presented. Assuming that the target is aligned planar and not occluded, the whole method can be divided into five steps:

(1) *Target extraction*: Extracts a region of interest around a starting point given near the reflection center (m, n). The region of interest depends on the resolution and the size of the target. Therefore, the distance between the sensor and the target has to be known.
(2) *Image standardization*: The region of interest will have different sizes (depending on its distance to the sensor). This step normalizes the region of interest to standardize some parameters and makes the following steps independent from the resolution and distance.
(3) *Cross-correlation*: This step detects the center of the target with pixel accuracy and is based on the cross-correlation approach presented in Section 2.
(4) *Sub-pixel approximation*: Sub-pixel accuracy is achieved by approximating the local neighborhood around the peak value of the cross-correlation by quadratic polynomials.

    The sub-pixel detection of the target center finishes with this step. However, contrarily to many other vision based sensors, laser scanners measure beside reflectance data also range data:
(5) *Projection to 3D*: To calculate the target center in 3D we first fit the 3D coordinates of the neighborhood around the target-center to a plane and then project the target-center to this plane.

3.1. Target extraction

The region of interest depends on the resolution and the size of the target. Therefore, the distance between the sensor and the target has to be known. In many imaging sensors like cameras there is no range infor-

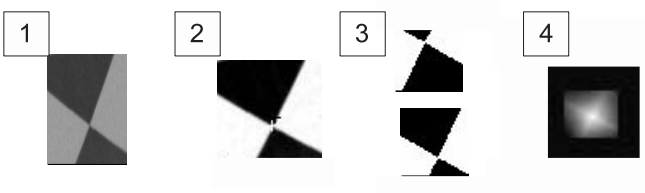

Figure 5: The figure shows the different steps of the method: (1) the input image G, (2) the scaled and enhanced image G_s, (3) the sub images H and $\tilde{H}^*$, and (4) the feature image C after the cross-correlation.

mation available. Then the definition of the size of the region of interest is done by experience.

However, our sensor has additionally to image information also range information, and thus the 3D coordinate of each pixel (i, j). Assume that we have a starting point (p, q) of an image R describing approximately the position of the target and that we know for each pixel (i, j) its distance to the sensor $d(i, j)$. Then we can define a set of pixel indices of R through

$$I_r := \{(i, j) \in N \times M \mid \|d(i, j) - d(p, q)\|_2 < r\} \quad (12)$$

with $2r$ giving the diameter of the target. So we get the region of interest of R (see Figure 5 (1)) through

$$G := (R(i, j))_{(i,j) \in I_r}. \quad (13)$$

3.2. Image standardization

The dimension (w, h) of G depends on its distance to the origin of the sensor, its resolution and the target-size. For implementation conveniences, we re-scale G to a *standardized image geometry* with width $\tilde{w}$ and height $\tilde{h}$ by re-sampling each pixel through the linear transformation

$$(i, j) := \left(\frac{u}{w}\tilde{w}, \frac{v}{h}\tilde{h}\right) \quad (14)$$

and call this resampled image G_r.

Denote the upper and lower 5% quantile of the histogram of G_r with $q_{\min}$ and $q_{\max}$. Outliers have a large influence on correlation based approaches. Therefore, we use the quantiles as upper and lower bounds to detect outliers and to reduce noise. We *standardize the image gray-values* by

$$G_s(u, v) := \frac{G_r(u, v) - q_{\min}}{q_{\max} - q_{\min}} \quad (15)$$

and call this standardized image G_s (see Figure 5 (2)).

3.3. Cross-correlation

G_s is now independent from its distance to the sensor and its resolution and is the input image for the algorithm like it was explained in Section 2. As shown in this section, we get the center (m, n) of the target with pixel accuracy (see Figure 5 (3) and 5 (4)).

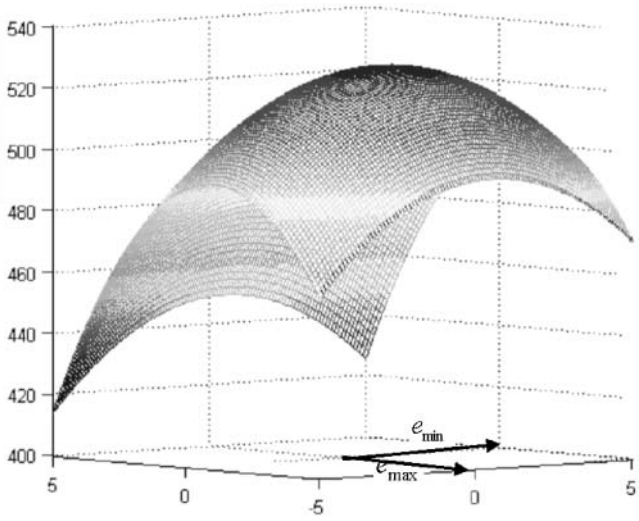

Figure 6: The figure shows the polynomial p and the direction of the eigenvalues of its Hessian.

3.4. Sub-pixel approximation

To achieve subpixel accuracy, many approaches apply 'least squares images matching' techniques (see Gruen 1985, Ackermann 1984), as they can compensate affine distortions and radiometric differences between correlation-patches. However, as in our approach the correlation-patches are derived from the same image (and are consequently not distorted and do not differ in radiometry), we do not benefit from this larger complexity.

In our approach, we achieve sub-pixel accuracy by reconstructing the local neighborhood around the pixel (m, n) of the feature image C of (10) with polynomials of degree 2. This approximation is very robust and accurate as the correlation image C has only one maximum (see Figure 5 (4)).

Denote $N_q(m, n) := \{(m - q, n - q), \ldots, (m + q, n + q)\}$ the $2q + 1$ neighborhood around the pixel (m, n), and denote

$$p(x, y) := a_0 + a_1 x + a_2 y + a_3 x^2 + a_4 y^2 + a_5 xy \quad (16)$$

a polynomial of degree 2 with the unknowns a_i. Then we minimize

$$\sum_{(u,v) \in N_q} (p(u, v) - C(u, v))^2 \to \min. \quad (17)$$

This optimization problem can be solved for $q \geq 1$ with a standard linear least squares approach.

To calculate the extremum of p we look onto the directions of its largest and smallest change in its curvature: These directions can be calculated by solving the eigenvectors $e_{\min}$ and $e_{\max}$ of the hessian of p (see Figure 6)

$$\text{hess}_p := \begin{pmatrix} \frac{p}{dx^2} & \frac{p}{dx\,dy} \\ \frac{p}{dx\,dy} & \frac{p}{dy^2} \end{pmatrix}. \quad (18)$$

The projection of p onto $e_{\min}$ results in a polynomial $q(x) := b_0 + b_1 x + b_2 x^2$ in one dimension whose extremum x_0 can be solved analytically. So the maximum in this direction is defined through $(m_0, n_0) := x_0 e_{\min}$. Similarly we get the projection of p onto $e_{\max}$ and call its maximum (m_1, n_1). So the overall maximum is defined through $(\tilde{m}, \tilde{n}) := (m, n) + (m_0, n_0) + (m_1, n_1)$.

3.5. Projection to 3D

Till this point, the position of the target center and thus its direction in 3D space is well reconstructed, however the range is not. To calculate the 3D coordinate of the target center $(\tilde{m}, \tilde{n})$, we transform the neighborhood I_r (see above) around the target center into 3D space and approximate these 3D coordinates $\{X_0, \ldots, X_n\}$ with a plane: denote the hessian normal form of the plane with its normal vector n and its distance to the origin d with $\langle n, X \rangle = d$. Then we solve

$$\sum_{i \in I} (\langle n, X_i \rangle - d) \rightarrow \min \tag{19}$$

with a standard approach. Now denote the 3D coordinate of the target center with $\tilde{X}$. Then, we interpret $\tilde{X}$ as a ray $t\tilde{X}$ $(t \in \mathbb{R})$ and calculate the intersection between $t\tilde{X}$ and the plane. It can easily be seen that the intersection P between $t\tilde{X}$ $(t \in \mathbb{R})$ and the plane is then calculated through

$$P := \tilde{X} \frac{d}{\langle n, \tilde{X} \rangle}. \tag{20}$$

4. Experimental results

In this section we show our experimental results and start with a short description of our hardware and setup.

4.1. System description and acquisition-setup

In our experiments we use the Z+F Imager 5006 (see Figure 1 (a)). The scanner consists of a range measurement system in combination with a mirror deflection device. The deflection system points the laser beam into the direction of measurement, the laser beam is emitted and then the reflected laser light is detected. A full panoramic scan is acquired by two rotations: The first rotates the mirror around a horizontal axis and thus deflects the laser beam in a vertical plane, whereas the second rotation is around the vertical center axis of the system. The current direction of the laser beam is measured by two encoders: One describes the current horizontal rotation and is adjusted at the center axis. The other one describes the mirror rotation and is adjusted along the mirror rotation axis. The result of each scan are two images: One image contains the reflectance values of the scanned area, with each pixel corresponding to a vertical and horizontal encoder value, whereas the second image – the range image – contains the range values. The scanning mode for our experiments has a spatial point distance of 6.4 mm in 10 m. For more information about the principle of the scanner see Abmayr et al. (2005).

4.2. Results

We did four different tests to prove the accuracy and stability of our method. In all tests we used the type of target as shown in Figure 1 (b) and with which we proved the symmetric property under perspective projection. All tests were done with the same implementation, without changing any parameter.

Stability test. To prove the stability and repeatability we scanned the same target in two different positions, the first position was at 8 m distance, the second position at 4 m distance. After scanning each position more than 800 times, we calculated some statistical parameters, like the mean and the RMS errors. Then we compared our method with a gradient based approach (in this case we replaced the steps described in Section 3.3 and Section 3.4 by the method implemented in the computer vision library *OpenCV*). As shown in Figure 8, our method is at least as stable as the method used by the computer vision library OpenCV and in some cases much more accurate. Figure 7 also illustrates the high repeatability and stability of our approach.

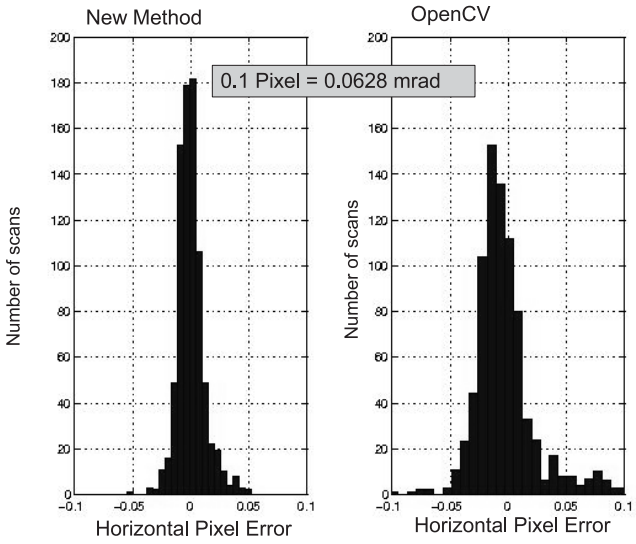

Figure 7: Target finder results of the first position in 8 m distance.

	"Symmetric Target"	"OpenCV"
Position 1	0.0116 mrad RMS	0.0324 mrad RMS
Position 2	0.0179 mrad RMS	0.0178 mrad RMS

Figure 8: The horizontal RMS error of the novel method as well as of the approach realized in the computer vision library of Intel (Intel 2005).

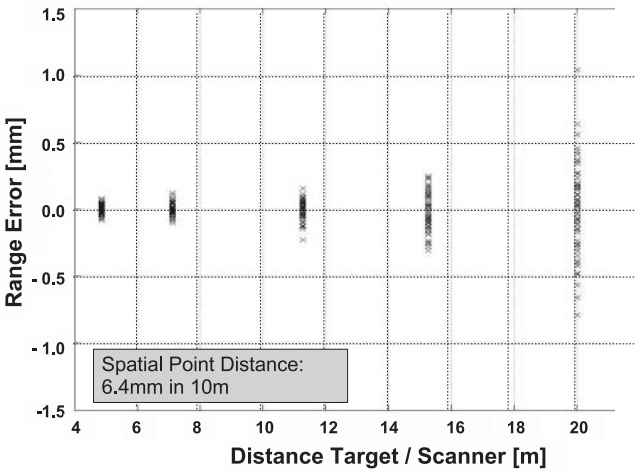

Figure 9: Remaining range error with respect to different ranges.

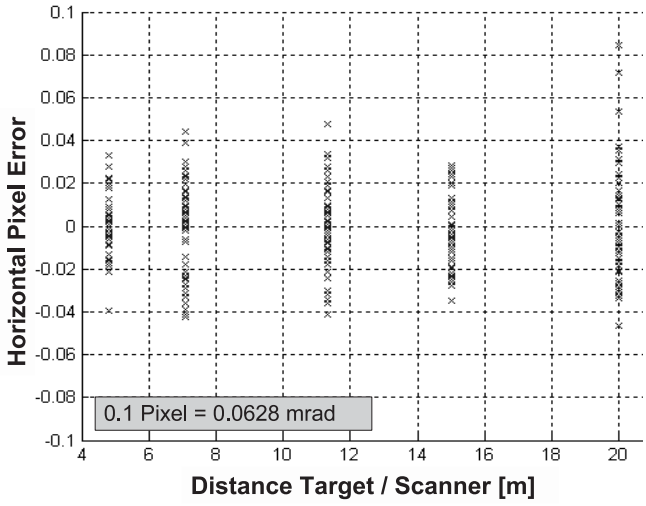

Figure 10: Remaining horizontal pixel error with respect to different ranges.

Distance test. In this experiment we scanned the target distances between 4.8 and 20 m and took about 50 scans in each position. This test shows that our approach is highly accurate to a wide variety of different ranges. Figure 9 shows the remaining range error and Figure 10 the remaining pixel error.

Translation test. In this experiment we demonstrate that the convergence of the method is not influenced by sampling effects. Therefore, we adjusted the target on a translation device, which enabled us to move the target laterally in 0.25 millimeter steps. We took about 30 scans of each position. To get the distance of the calculated target centers from the ideal position, we fitted a line through the resulting center points with respect to the translation of the target. Then we calculated the distance of the fitted line to each target center. The results are shown in Figure 11 and demonstrate that our method succeeds independently of the sampling position of the laser beam.

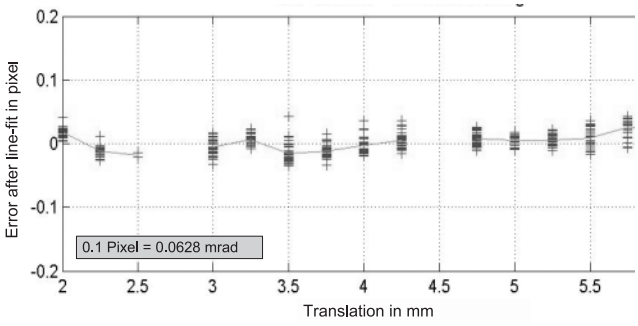

Figure 11: Remaining error after a line-fit with respect to the offset of the translation device.

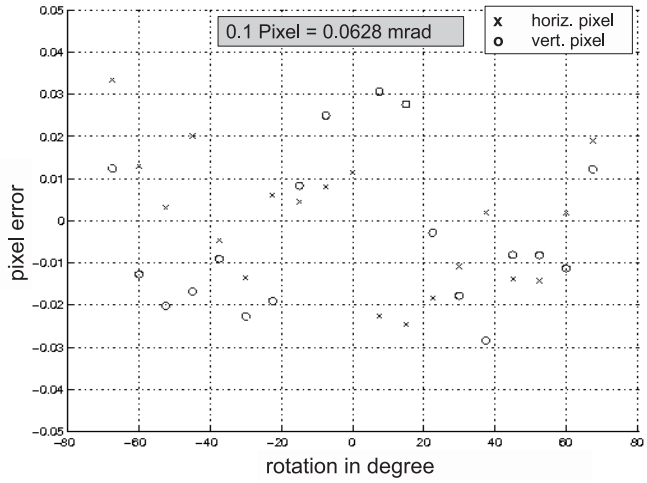

Figure 12: Remaining pixel error of the simulated target with respect to the rotation of the target.

Rotation test. As this test was difficult to realize in practice, we simulated the target by using the function shown in (21) (see Appendix). To become more realistic, we added gaussian noise to it. Then we applied off-plane rotation around the target center in steps of 7.5 degree in a range of -67.5 degree to 67.5 degree. The result (see Figure 12) proves the applicability of our method with respect to rotation.

5. Discussion and outlook

The approach presented in this paper is highly accurate and robust, but even so takes into account the special conditions which many applications in terrestrial laser scanning have to face: Invariance to perspective projections and rotation, as well as a high degree of robustness to different distances and resolutions.

The basic idea i.e. the use of symmetric structures in targets can also be applied in 3D space. In a next step, we will modify our approach to work consequently in 3D, without projecting the data perspec-

tively. Furthermore, the correlation based character could be used for quality control.

To date, the method is validated and used in many calibration and field applications. Being developed and optimized for laser scanner data, the basic steps are vision based and therefore should also work on other types of optical sensors.

Acknowledgments

We thank the laser team of Zoller+Fröhlich GmbH for their excellent research work and support on the Imager 5006. We also thank M. Suppa, H. Hirschmüller and all other involved colleagues from the Institute of Robotics and Mechatronics at the German Aerospace Center as well as Prof. Staiger from the Fachhochschule Bochum for the good cooperation. This work was partly funded by the DFG project "Canopy Analyser".

Appendix

In this section we catch up the proof, that the chesspattern type shown in Figure 4 holds the symmetry property of Section 2.1 also under perspective projection.

Let $\tilde{u} = (\tilde{u}_1, \tilde{u}_2, \tilde{u}_3)$ and $\tilde{v} = (\tilde{v}_1, \tilde{v}_2, \tilde{v}_3)$ be two non-collinear vectors in 3D space, $\tilde{m} = (\tilde{m}_1, \tilde{m}_2, \tilde{m}_3) \in \mathbb{R}^3$ the center of the target and $\times$ the cross product (see Figure 4). Set $a := \tilde{u} - \tilde{m}$, $b := \tilde{v} - \tilde{m}$, $A_x := \tilde{x} - \tilde{m}$ and define a 3D target as the set of points which holds

$$\tilde{T} := \{\tilde{x} \in \mathbb{R}^3 : (a \times A_{\tilde{x}})(b \times A_{\tilde{x}}) \geq 0\} \qquad (21)$$

and define the perspective projection P for any $\tilde{x} = (\tilde{x}_1, \tilde{x}_2, \tilde{x}_3) \in \mathbb{R}^3$ with $\tilde{x}_3 \neq 0$ through $P(\tilde{x}) := \left(\frac{\tilde{x}_1}{\tilde{x}_3}, \frac{\tilde{x}_2}{\tilde{x}_3}\right)$. Then

$$T := P(\tilde{T}) \qquad (22)$$

defines a symmetric target.

Proof. To show that T is a symmetric target take any $x \in T$ and set $m := P(\tilde{m})$, $u := P(\tilde{u})$ and $v := P(\tilde{v})$ and set

$$s := ((u - m) \times (x - m))((v - m) \times (x - m)). \qquad (23)$$

We have to show that $A_m(x) \in T$. For this set $y := A_m(x)$ and we get

$$q := ((u - m) \times (y - m))((v - m) \times (y - m)) \qquad (24)$$

which can with (2) be simplified to $q = ((u - m) \times (m - x))((v - m) \times (m - x))$. But now $q = s$ and thus $y \in T$. □

References

Abmayr, T., Dalton, G., Härtl, F., Hines, D., Liu, R., Hirzinger, G., and Fröhlich, C., Standardisation and visualization of 2.5D scanning data and rgb color information by inverse mapping, 7th Conference on Optical 3D Measurement Techniques, Vienna, Austria (2005).

Ackermann, F., Digital Image Correlation: Performance and potential application in photogrammetry, Photogrammetric Record 11 (64) (1984), 429–439.

Bookstein, F. L., Fitting conic sections to scattered data, Comput. Vision, Graphics and Image Processing 9 (1988), 56–71.

Fitzgibbon, A. W. and Fisher, R., A Buyer's guide to conic Fitting, Proceedings, 5th Brithish Machine Vision Conference, Birmingham (1995), pp. 513–522.

Förstner, W. and Gülch, E., A fast operator for detection and precise location of distinct points, corners and centers of circular features, Proceedings, ISPRS Intercommission Workshop on Fast Processing of Photogrammetric data (1987).

Gruen, A., Adaptive least squares correlation: A powerful image matching technique, S Afr J of Photogrammetry, Remote Sensing and Cartography 14:3 (1985), pp. 175–187.

Harris, C. and Stephens, M., A combined corner and edge detector, Proceedings, 4th Alvey Vision Conference, Manchester (1988), 147–151.

Hirzinger, G., Bodenmüller, T., Hirschmüller, H., Liu, R., Sepp, W., Suppa, M., Abmayr, T., and Strackenbrock, B., Photo-realistic 3D modelling—From robotics perception towards cultural heritage. International Workshop on Recording, Modeling and Visualization of Cultural Heritage, Ascona, Switzerland, May 22–27, 2005.

Intel, Open Computer Vision Library, http://www.intel.com (2005).

Shi, J. and Tomasi, C., Good features to track, Proceedings, IEEE Conference on Computer Vision and Pattern Recognition (CVPR94), Seattle (1994).

Received: Mar 05, 2008 Accepted: May 21, 2008

Author information
Thomas Abmayr, Franz Härtl and Christoph Fröhlich
Zoller+Fröhlich GmbH
Simoniusstr. 22
88239 Wangen, Germany
E-mail: t.abmayr@zofre.de, fh@zofre.de, info@zofre.de

Darius Burschka
Technical University of Munich
Boltzmannstr. 3
85748 Garching, Germany
E-mail: burschka@cs.tum.edu

Gerd Hirzinger
Institute of Robotics and Mechatronics
German Aerospace Center
Münchner Str. 20
82234 Oberpfaffenhofen-Wessling, Germany
E-mail: gerd.hirzinger@dlr.de